https://ntrs.nasa.gov/search.jsp?R=19820012309 2020-03-21T08:40:12+00:00Z

NASA
TP
1987
c.1

NASA
Technical
Paper
1987

March 1982

Damping Seals for Turbomachinery

George L. von Pragenau

TECH LIBRARY KAFB, NM
0068150

LOAN COPY
AFWL TECHNICAL LIBRARY
Kirtland AFB, N. M.

NASA

TECH LIBRARY KAFB, NM
0068150

NASA Technical Paper 1987

1982

Damping Seals for Turbomachinery

George L. von Pragenau
George C. Marshall Space Flight Center
Marshall Space Flight Center, Alabama

NASA
National Aeronautics and Space Administration

Scientific and Technical Information Branch

TABLE OF CONTENTS

LIST OF ILLUSTRATIONS

LIST OF TABLES

LIST OF SYMBOLS

a	gap velocity effect, Eq. (83)
A	relative seal gap velocity, Eq. (43)
a_o	unit matrix constant, Eq. (91)
b	gap acceleration effect, Eq. (79)
B	relative seal gap acceleration, Eq. (56)
b_o	right angle rotation matrix constant, Eq. (91)
c	Couette factor, Fig. 3 and Eq. (42)
C	induced seal damping, Eq. (103)
C_c	whirl coupling, Eq. (105)
C_o	steady-state induced seal damping, Eq. (100)
d	inlet effect, Eq. (77)
D	determinants, Eqs. (6) and (110)
e	relative eccentricity, Eqs. (1) and (18)
E	relative gap change, Eq. (19)
f	pipe friction factor
f_r	rotor friction, Eq. (29)
f_{re}	expanded rotor friction, Eq. (31)
f_s	stator friction, Eq. (28)
f_{se}	expanded stator friction, Eq. (30)
f_1	inlet loss factor, Eq. (60)
f_2	outlet loss factor, Eq. (61)
F	combined friction effect, Eq. (49)
F_y	force component in y, Eqs. (1) and (107)
F_z	force component in z, Eqs. (1) and (107)

g_r	rotor friction velocity effect, Eq. (33)
g_s	stator friction velocity effect, Eq. (32)
G	additive friction velocity effect, Eq. (50)
h	radial seal gap, Eq. (18)
h_o	average radial seal gap, Eqs. (1) and (18)
h_r	rotor friction gap effect, Eq. (35)
h_s	stator friction gap effect, Eq. (34)
H	additive friction gap effect, Eq. (51)
i	2X1 unit vector, Eq. (3)
I	2X2 unit matrix, Eq. (12)
k_r	rotor surface roughness, Eq. (29)
k_s	stator surface roughness, Eq. (28)
K	induced seal stiffness, Eq. (102)
K_g	generalized modal stiffness, Eq. (108)
K_o	steady-state induced seal stiffness, Eq. (99)
K_r	resultant stiffness, Eq. (108)
K_y	suspension stiffness in y, Eq. (4) and Fig. 1
K_z	suspension stiffness in z, Eq. (4) and Fig. 1
L	seal gap length, Eq. (59)
m	induced seal mass, Eq. (104)
m_c	whirl rate coupling, Eq. (106)
m_g	generalized modal mass, Eq. (109)
m_o	steady-state induced seal mass, Eq. (101)
m_r	resultant mass, Eq. (109)
m_s	simple model rotor mass, Fig. 1
N	inlet coupling transfer function, Eq. (74)

p	seal gap pressure, Eq. (58)
p_a	average seal gap pressure, Eq. (73)
p_o	inlet cavity pressure, Eq. (60)
p_1	gap inlet pressure, Eq. (58)
p_2	gap outlet pressure, Eq. (59)
p_3	outlet cavity pressure, Eq. (61)
q	circumferential coordinate, Eq. (20)
Q	rotation matrix for angle β-α, Eq. (11)
Q_α	rotation matrix for angle α, Eq. (2)
Q_β	rotation matrix for angle β, Eq. (90)
r	rotor radius, Fig. 2
R	stator radius, Fig. 2
R_r	Reynolds number relative to rotor, Eq. (27)
R_s	Reynolds number relative to stator, Eq. (26)
s	Laplace operator
t	time
T	transpose of vectors and matrices, Eqs. (13) and (89)
u	axial bulk flow velocity, Fig. 2
u_a	average axial bulk flow velocity at gap inlet, Eq. (63)
u_b	variable axial bulk flow velocity at gap inlet, Eq. (63)
u_1	gap inlet axial bulk flow velocity, Eq. (44)
v	Couette flow velocity, Fig. 2
w	rotor surface velocity, Fig. 2
x	axial coordinate, Fig. 2
y	first radial coordinate, Fig. 1
z	second radial coordinate, Fig. 1

α	rotor whirl angle, Fig. 2
β	gap position angle, Fig. 2
$\dot{\gamma}$	relative whirl angle rate, Eq. (42)
Δ	difference, Eq. (52)
μ	viscosity, Eq. (26)
ρ	density, Eq. (22)
τ	gap flow time constant, Eq. (68)
τ_a	damping lead time constant, Eq. (84)
τ_b	mass lead time constant, Eq. (80)
τ_o	time constant limit, Eq. (69)
τ_r	shear stress on rotor, Eq. (23)
τ_{rq}	circumferential shear stress on rotor, Eq. (25)
τ_{rx}	axial shear stress on rotor, Eq. (24)
τ_s	shear stress on stator, Eq. (22)
τ_{sq}	circumferential shear stress on stator, Eq. (25)
τ_{sx}	axial shear stress on stator, Eq. (24)
τ_u	upper time constant limit, Eq. (85)
ω	circular frequency, Eq. (102)
ω_o	critical speed in radien/s, Eqs. (7) and (111)
Ω	rotor speed in radien/s, Eqs. (1) and (42)
Ω_L	rotor speed limit in radien/s, Eq. (114)
Π	right angle rotation matrix, Eq. (12)

TECHNICAL PAPER

DAMPING SEALS FOR TURBOMACHINERY

INTRODUCTION

The stable operation of turbomachinery depends mainly on the damping of the rotor motion [1]. Squeeze film dampers are designed for this very purpose [2], and also shaft seals are employed [3,4]. Seals are most convenient, since they are already included in the turbomachine design. However, the damping of a seal also generates a whirl driver force as shown in the pioneering work of Henry Black [5] who died January 17, 1980. He and his service to all are well-remembered [6].

The seal damping, normally effective only to twice the first critical speed, becomes an unstable whirl driver at higher speeds. Thus, high performance turbomachinery which has to run above the first critical speed is limited by an upper bound twice the first critical speed unless additional damping is applied. The fluid shear forces between the rotating journal and the stationary bushing produce a circumferential bulk flow, known as Couette flow [7], at half the shaft speed. The fundamental relation between Couette flow and whirl forces was recognized by Black [5]. Black, Allaire, and Barrett [8] found for the circumferential flow, as an approximation, an exponential function with the axial position as the independent variable, the inlet swirl as the boundary condition, and the Couette flow at half speed as the asymptote. It is shown that the whirl force can be reduced with a low or reversed inlet swirl under the assumption that the swirl can be transferred from the inlet cavity to the narrow seal gap.

This paper proposes the application of the seal surface roughness for stabilization and sealing. The distribution of the circumferential flow is approximated by the asymptotic state of the Couette flow which is assumed to prevail over the total seal length. The approximation is justified by the results of Black et al. [8], who show that seal friction advances the asymptotic approach upstream toward the inlet. The formulation treats the Couette flow generation by surfaces of different roughness without invoking a dominant axial flow as in References 5 and 8. This generalization is more representative of long seals. The turbulent seal friction is given by Moody's pipe friction formula [9] for Reynolds numbers up to 10^5 and above. Linearization is applied at the steady flow point to aid the integration of the flow effects over the cylindrical surfaces. The steady flow is determined with the Newton-Raphson's iteration method. The dynamic parameters are derived for small deflections about the seal's center position. Numerical results are given for the oxygen and the hydrogen turbopumps of the Space Shuttle main engine.

ROTOR STABILITY

This section briefly reviews the purpose of the rotor damping with the help of a simple model. The model consists of a rotor (Fig. 1) with a mass m_s, eccentricity eh_o, combined bearing and seal stiffnesses K_y and K_z, seal damping C, speed Ω, and Couette flow velocity v. The whirl cross coupling is given by $c\Omega C = (v/r)C$, with the Couette factor c and the seal radius r. The centrifugal force caused by the unbalance is given in equation (1). The components of the force are obtained with matrix Q_α of the equation (2) that rotates the unit vector i of equation (3) by the angle α. The force is balanced by the dynamic stiffness effect given in equation (4). The inverse is the response of equation (5).

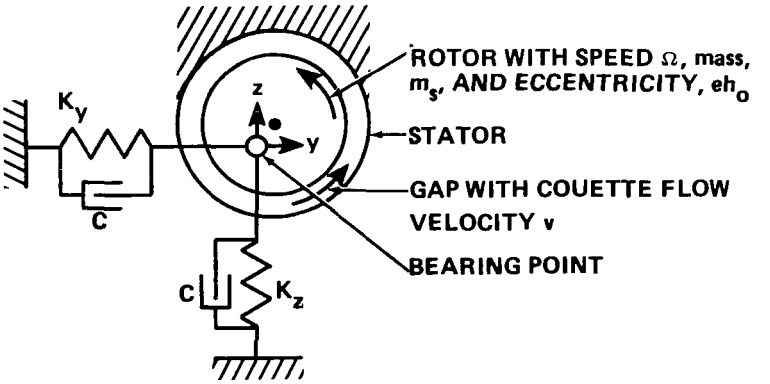

Figure 1. Simple rotor model.

$$\begin{bmatrix} F_y \\ F_z \end{bmatrix} = eh_o m_s \Omega^2 Q_\alpha i \tag{1}$$

$$Q_\alpha = \begin{bmatrix} \cos\alpha & -\sin\alpha \\ \sin\alpha & \cos\alpha \end{bmatrix} \tag{2}$$

$$i = \begin{bmatrix} 1 \\ 0 \end{bmatrix} \tag{3}$$

$$\begin{bmatrix} F_y \\ F_z \end{bmatrix} = \begin{bmatrix} K_y + sC + s^2 m_s & c\Omega C \\ -c\Omega C & K_z + sC + s^2 m_s \end{bmatrix} \begin{bmatrix} y \\ z \end{bmatrix} \tag{4}$$

$$\begin{bmatrix} y \\ z \end{bmatrix} = \begin{bmatrix} K_z + sC + s^2 m_s & -c\Omega C \\ c\Omega C & K_y + sC + s^2 m_s \end{bmatrix} \begin{bmatrix} F_y \\ F_z \end{bmatrix} \frac{1}{D} \tag{5}$$

$$D = K_y K_z + (c\Omega C)^2 + sC(K_y + K_z) + s^2 [C^2 + m_s(K_y + K_z)] + s^3 2Cm_s + s^4 m_s^2 \tag{6}$$

The common denominator of equation (5), given in equation (6), results from the determinant of equation (4). The characteristic equation D = 0 determines the stability. The mapping of the contour of the right half of the complex s-plane (see Nyquist criterion [10]) yields the stability criterion. The limit is found by rearranging equation (6) for $s = j\omega$ and setting D = 0. The imaginary part of D yields the critical speed and rotor resonance [Eq. (7)]; and the real part of D, the stability limit (inequalities 8 to 10).

$$\omega_o = \sqrt{(K_y + K_z)/2m_s} \tag{7}$$

$$K_y K_z + (c\Omega C)^2 + (K_y + K_z)^2/4 < \frac{K_y + K_z}{2m_s} [C^2 + m_s(K_y + K_z)] \tag{8}$$

$$(c\Omega C)^2 < C^2 \frac{K_y + K_z}{2m_s} + \frac{(K_y - K_z)^2}{4} \tag{9}$$

$$\Omega < \omega_o/c \tag{10}$$

The stability condition of inequality (9) is obtained by rearranging the inequality (8). The special case of a uniform suspension ($K_y = K_z$) yields the simplest stability criterion : inequality (10). The latter satisfies also the inequality (9) on the conservative side. Inequality (10) limits the speed of turbomachinery that operates above the critical speed. For example, a half-speed Couette flow has a c = 0.5 and limits the speed at twice the critical speed ($\Omega < 2\omega_o$) as, e.g., early in the development of the high pressure hydrogen turbopump of the Space Shuttle main engine [4]. If the Couette flow has a c = 0.25, then the limit is extended to $\Omega < 4\omega_o$. The objective of this study is to define a seal configuration with a Couette factor $c < 0.5$.

SEAL GEOMETRY

Figure 2 shows the cross section of the seal for an exaggerated gap situation. The eccentricity eh_o ($0 < e < 1$) points with the time dependent angle $\alpha(t)$, and the gap is measured at an angle β. Both angles are inertially referenced. The cylindrical coordinates are x (axial position) and $q = r\beta$ ($r \doteq R$ circumferential position). Equations (11) through (15) give, in respective order, the rotational transformation matrix Q for the angle β-$\alpha(t)$, the right angle rotation matrix Π, the unit vector i, the partial derivative after β, and the partial derivative after time. Equations (16) through (21) are, in respective order, the compact expressions of cosine and sine, seal gap h, the differential relative to the gap, the circumferential partial derivative relative to the gap, and the time partial derivative relative to the gap. Equation (18) follows from Figure 2, $R - r = h_o$, $R \doteq r$, and $h \doteq R - [r + eh_o\cos(\beta - \alpha)] = h_o[1 - e\cos(\beta - \alpha)]$.

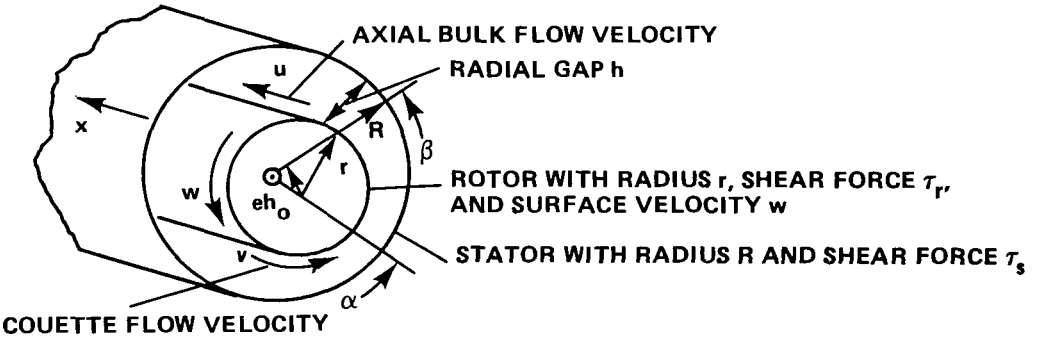

Figure 2. Seal cross section.

$$Q = \begin{bmatrix} \cos(\beta-\alpha) & -\sin(\beta-\alpha) \\ \sin(\beta-\alpha) & \cos(\beta-\alpha) \end{bmatrix} \tag{11}$$

$$\Pi = \begin{bmatrix} 0 & -1 \\ 1 & 0 \end{bmatrix}, \quad I = \begin{bmatrix} 1 & 0 \\ 0 & 1 \end{bmatrix} = -\Pi^2 \tag{12}$$

$$i = \begin{bmatrix} 1 \\ 0 \end{bmatrix}, \quad i^T = [1 \quad 0] \tag{13}$$

$$\frac{\partial Q}{\partial \beta} = \Pi Q \tag{14}$$

$$\frac{\partial Q}{\partial t} = -\dot{\alpha}\Pi Q \tag{15}$$

$$\cos(\beta-\alpha) = i^T Q i \tag{16}$$

$$\sin(\beta-\alpha) = -i^T \Pi Q i \tag{17}$$

$$h = h_o(1 - e i^T Q i) \tag{18}$$

$$\frac{dh}{h_o} = -e i^T Q i = -E \tag{19}$$

$$\frac{1}{h_o}\frac{\partial h}{\partial q} = \frac{-e}{r} i^T \Pi Q i \tag{20}$$

$$\frac{1}{h_o}\frac{\partial h}{\partial t} = -i^T(\dot{e}I - \dot{\alpha}e\Pi)Qi \tag{21}$$

FLOW FRICTION

The flow friction is given by the pressure drop in pipes $\Delta p = \rho(u^2/2)(L/D)f$ with the friction factor f [9], length L, hydraulic diameter D (D = 2h for seals with radial gap h), roughness κ (k/h roughness relative to gap h), axial bulk flow velocity u, and fluid density ρ [11]. The seal has the axial and circumferential bulk flow velocities u and v and the rotor surface velocity w (Fig. 2). The fluid shear stresses on the surfaces of the stator (bushing) and the rotor (journal) are τ_s in equation (22) and τ_r in equation (23). The pressure gradient is given in equations (24) and (25) with the axial and circumferential components. The Reynolds

numbers are given in equations (26) and (27), the frictions in equations (28) and (29), the friction's Taylor expansions in equations (30) and (31), the friction velocity factors in equations (32) and (33), and the friction gap factors in equations (34) and (35); all equation pairs are for the stator and rotor, respectively. The fluid viscosity is μ in equations (26) and (27) and the surface roughnesses k_s and k_r in equations (28), (29), and (32) through (35) for the stator and rotor, respectively.

$$\tau_s = \rho \frac{u^2+v^2}{2} \cdot \frac{f_s}{4} \tag{22}$$

$$\tau_r = \rho \frac{u^2+(v-w)^2}{2} \cdot \frac{f_r}{4} \tag{23}$$

$$\frac{-\partial p}{\partial x} = \frac{\tau_{sx}+\tau_{rx}}{h} = \frac{\rho}{8h}\left[uf_s\sqrt{u^2+v^2} + uf_r\sqrt{u^2+(v-w)^2}\right] \tag{24}$$

$$\frac{-\partial p}{\partial q} = \frac{\tau_{sq}+\tau_{rq}}{h} = \frac{\rho}{8h}\left[vf_s\sqrt{u^2+v^2} + (v-w)f_r\sqrt{u^2+(v-w)^2}\right] \tag{25}$$

$$R_s = \frac{\rho}{\mu} 2h\sqrt{u^2+v^2} \tag{26}$$

$$R_r = \frac{\rho}{\mu} 2h\sqrt{u^2+(v-w)^2} \tag{27}$$

$$f_s = 0.0055\left[1+\left(10^4 \frac{k_s}{h} + \frac{10^6}{R_s}\right)^{1/3}\right] \tag{28}$$

$$f_r = 0.0055\left[1+\left(10^4 \frac{k_r}{h} + \frac{10^6}{R_r}\right)^{1/3}\right] \tag{29}$$

$$f_{se} = f_s - g_s \frac{udu+vdv}{u^2+v^2} - h_s \frac{dh}{h} \tag{30}$$

$$f_{re} = f_r - g_r \frac{udu+(v-w)dv}{u^2+(v-w)^2} - h_r \frac{dh}{h} \tag{31}$$

$$g_s = \frac{0.0055 \cdot 10^6}{3R_s(10^4 k_s/h + 10^6/R_s)^{2/3}} \tag{32}$$

$$g_r = \frac{0.0055 \cdot 10^6}{3R_r(10^4 k_r/h + 10^6/R_r)^{2/3}} \tag{33}$$

$$h_s = \frac{0.0055}{3} (10^4 k_s/h + 10^6/R_s)^{1/3} \tag{34}$$

$$h_r = \frac{0.0055}{3} (10^4 k_r/h + 10^6/R_r)^{1/3} \tag{35}$$

COUETTE FLOW

The Couette flow is generated by the rotor shear force and resisted by the stator shear force. An eccentricity causes an additional circumferential flow that produces the pressure gradient component of equation (25). The latter is assumed to be negligible, as expressed by the equation (36), which yields the Couette factor c = v/w. The limits given in equations (37) and (38) follow from the circumferential and the axial flow dominances. The Couette factor varies little with u, as Figure 3 shows.

$$v f_s \sqrt{u^2+v^2} + (v-w) f_r \sqrt{u^2+(v-w)^2} = 0 \tag{36}$$

$$u = 0: \; c = \frac{v}{w} = 1/(1+\sqrt{f_s/f_r}) \tag{37}$$

$$u = \infty: \; c = \frac{v}{w} = 1/(1+f_s/f_r) \tag{38}$$

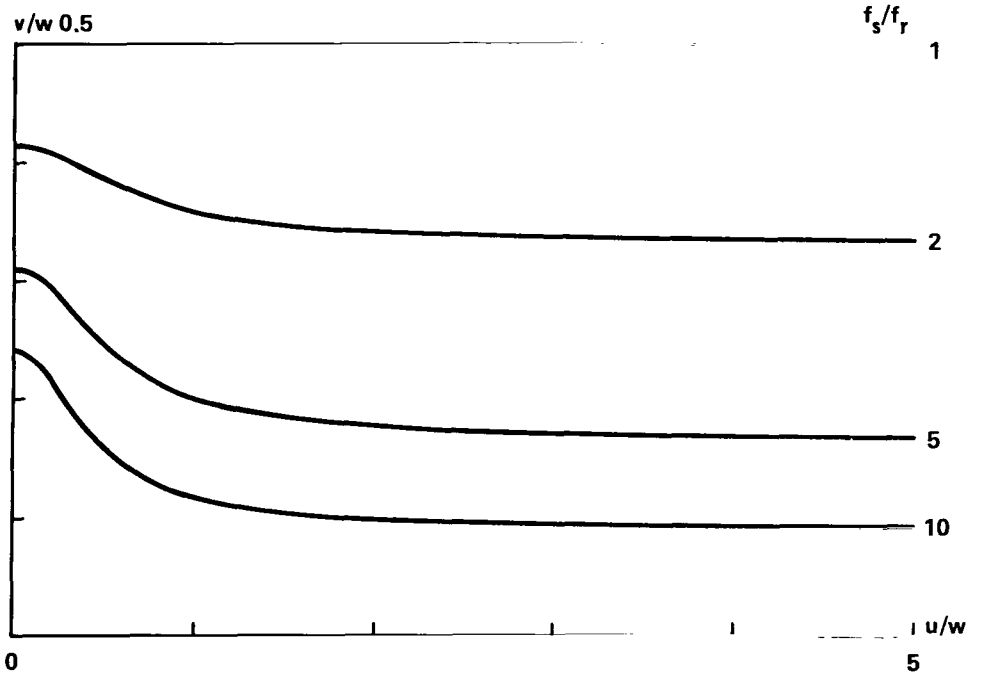

Figure 3. Couette factor c = v/w versus the axial flow velocity ratio u/w for friction ratios f_s/f_r.

FLOW CONTINUITY

The motion of the gap pumps the assumed incompressible fluid, according to equation (39), to preserve the volume. The equation is further simplified to equation (40) by canceling terms, assuming no gap taper ($\partial h/\partial x = 0$), and by assuming a constant circumferential flow ($\partial v/\partial q = 0$). Equation (41) is obtained by substituting equations (20) and (21) in equation (40), and by approximating $1/h$ with $1/h_o$. The introduction of the definitions of the equations (42) and (43) and the integration of equation (41) yield the axial velocity of equation (44) with u_1 as the inlet velocity.

$$uhdq + vhdx = uhdq + h\frac{\partial u}{\partial x}dxdq + vhdx + h\frac{\partial v}{\partial q}dqdx + v\frac{\partial h}{\partial q}dqdx + \frac{\partial h}{\partial t}dxdq \tag{39}$$

$$\frac{\partial u}{\partial x} + \frac{v\partial h}{h\partial q} + \frac{\partial h}{h\partial t} = 0 \tag{40}$$

$$\frac{\partial u}{\partial x} = i^T(\dot{e}I - \dot{\alpha}e\Pi)Qi + \frac{v}{r}ei^T\Pi Qi = A \tag{41}$$

$$\dot{\gamma} = \dot{\alpha} - \frac{v}{r} = \dot{\alpha} - c\Omega \tag{42}$$

$$A = i^T(\dot{e}I - \dot{\gamma}e\Pi)Qi \tag{43}$$

$$u = u_1 + xA \tag{44}$$

PRESSURE DISTRIBUTION

The dynamic pressure gradient of equation (45) follows from equation (24) by adding the mass acceleration of equation (46). The equation (47) is obtained by expanding all factors of equation (45) with first order terms and by utilizing the expanded friction factors of equations (30) and (31). The multiplication of all factors and the neglecting of second order terms yield equation (48), which is the Taylor expansion of equation (45). The definitions of equations (49) through (51) lead to the compact form of the Taylor expansion, equation (52). The time derivative of equation (46) applied to equation (44) yields equation (53). The definitions of equations (42) and (56) result in a further simplification, equation (54). The pressure distribution of equation (58) is obtained by integrating equation (52); by substituting the definitions of equations (19), (43), (55), and (56); and by employing the approximation of equation (57).

$$\frac{-\partial p}{\partial x} = \frac{\rho u}{8h}\left[f_s\sqrt{u^2+v^2} + f_r\sqrt{u^2+(v-w)^2}\right] + \rho\frac{du}{dt} \tag{45}$$

$$\frac{du}{dt} = \frac{\partial u}{\partial t} + u\frac{\partial u}{\partial x} + v\frac{\partial u}{\partial q} \tag{46}$$

$$\frac{-\partial p}{\partial x} = \frac{\rho u_1}{8h_o}\left(1+\frac{du}{u_1}-\frac{dh}{h_o}\right)\left[f_s\left(1-\frac{g_s}{f_s}\frac{u_1 du}{u_1^2+v^2}-\frac{h_s}{f_s}\frac{dh}{h_o}\right)\sqrt{u_1^2+v^2}\left(1+\frac{u_1 du}{u_1^2+v^2}\right)\right.$$

$$\left. + f_r\left(1-\frac{g_r}{f_r}\frac{u_1 du}{u_1^2+(v-w)^2}-\frac{h_r}{f_r}\frac{dh}{h_o}\right)\sqrt{u_1^2+(v-w)^2}\left(1+\frac{u_1 du}{u_1^2+(v-w)^2}\right)\right] + \rho\frac{du}{dt} \tag{47}$$

$$\frac{-\partial p}{\partial x} = \frac{\rho u_1}{8h_o}\left\{f_s\sqrt{u_1^2+v^2}\left[1+\frac{du}{u_1}\left(1+u_1^2\frac{1-g_s/f_s}{u_1^2+v^2}\right)-\frac{dh}{h_o}\left(1+\frac{h_s}{f_s}\right)\right]\right.$$

$$\left. + f_r\sqrt{u_1^2+(v-w)^2}\left[1+\frac{du}{u_1}\left(1+u_1^2\frac{1-g_r/f_r}{u_1^2+(v-w)^2}\right)-\frac{dh}{h_o}\left(1+\frac{h_r}{f_r}\right)\right]\right\} + \rho\frac{du}{dt} \tag{48}$$

$$F = \frac{\rho}{8h_o}\left[f_s\sqrt{u_1^2+v^2} + f_r\sqrt{u_1^2+(v-w)^2}\right] \tag{49}$$

$$G = \frac{\rho u_1^2}{8h_o}\left[\frac{f_s-g_s}{\sqrt{u_1^2+v^2}} + \frac{f_r-g_r}{\sqrt{u_1^2+(v-w)^2}}\right] \tag{50}$$

$$H = \frac{\rho}{8h_o}\left[h_s\sqrt{u_1^2+v^2} + h_r\sqrt{u_1^2+(v-w)^2}\right] \tag{51}$$

$$\frac{-\partial p}{\partial x} = u_1 F + (F+G)\Delta u_1 - \frac{dh}{h_o}u_1(F+H) + \rho\frac{du}{dt} \tag{52}$$

$$\frac{du}{dt} = \frac{du_1}{dt} + xi^T[(\ddot{e}-\dot{\alpha}\dot{\gamma}e)I - (\dot{\alpha}\dot{e}+\dot{\gamma}\dot{e}+\ddot{\alpha}e)\Pi]Qi + u\frac{\partial u}{\partial x} + xi^T\frac{v}{r}(\dot{\gamma}eI+\dot{e}\Pi)Qi \tag{53}$$

$$\frac{du}{dt} = \frac{du_1}{dt} + xi^T[(\ddot{e}-\dot{\gamma}^2 e)I - (\ddot{\alpha}e+2\dot{\gamma}\dot{e})\Pi]Qi + u\frac{\partial u}{\partial x} = \frac{du_1}{dt} + xB + u\frac{\partial u}{\partial x} \tag{54}$$

$$\frac{dh}{h_o} = -E \tag{19}$$

$$\Delta u_1 = u - u_1 = xA \tag{55}$$

$$B = i^T[(\ddot{e}-\dot{\gamma}^2 e)I - (\ddot{\alpha}e+2\dot{\gamma}\dot{e})\Pi]Qi \tag{56}$$

$$\frac{u^2 - u_1^2}{2} \doteq u_1(u-u_1) = u_1 xA \tag{57}$$

$$p_1 - p = xu_1F + \frac{x^2}{2}A(F+G) + xu_1E(F+H) + x\rho\frac{du_1}{dt} + \frac{x^2}{2}\rho B + x\rho u_1 A \tag{58}$$

BOUNDARY CONDITIONS

The pressure drop over the total seal gap length L of equation (59) follows from x = L in equation (58). The inlet loss f_1 reduces the inlet cavity pressure p_o to the inlet pressure p_1 of equation (60), assuming $u_o = 0$. The outlet pressure p_2 equals the outlet cavity pressure p_3 of equation (61), assuming a sudden discharge into a large outlet cavity ($f_2 = 1$) and $u_3 = 0$. Equation (62) gives the pressure drop from one to the other cavity. Equation (63) describes the inlet flow velocity u_1 as the sum of the steady (u_a) and the oscillatory (u_b) velocities. Equation (64) results from equations (62) and (63), $u_a >> u_b$, $u_1F \doteq u_aF + u_b(F+G)$, and from neglecting second order terms. The steady-state part of equation (64) is given in equation (65) as a Taylor expansion, and in equation (66) in the iterative form after Newton-Raphson. Equation (67) is the oscillatory component of equation (64) with s replacing $d(\cdot)/dt$ and tacitly assuming the Laplace transform for the variables. Equation (68) defines the time constant τ, and equation (69) the limit τ_o that is found by conservatively neglecting $\rho u_a(1+f_1)$. Equation (70) follows from equations (58) and (60). Equation (71) follows from equations (63) and (70), $u_a >> u_b$, $u_1^2/2 \doteq u_a^2/2 + u_a u_b$, $u_1F \doteq u_aF + u_b(F+G)$, and by neglecting second order terms. The pressure distribution of equation (71), together with equations (66) and (67), expresses the effects of the boundary conditions and the seal gap.

$$p_1 - p_2 = Lu_1F + Lu_1E(F+H) + \frac{L^2}{2}A(F+G) + L\rho\frac{du_1}{dt} + \frac{L^2}{2}\rho B + L\rho u_1 A \tag{59}$$

$$p_o - \rho\frac{u_1^2}{2}\cdot f_1 = p_1 + \rho\frac{u_1^2}{2} \tag{60}$$

$$p_2 + \rho \frac{u_2^2}{2} = p_3 + \rho \frac{u_2^2}{2} \cdot f_2 \quad , \quad f_2 = 1 \tag{61}$$

$$p_o - p_3 = p_1 - p_2 + \rho \frac{u_1^2}{2}(1+f_1)$$

$$= \rho \frac{u_1^2}{2}(1+f_1) + Lu_1F + Lu_1E(F+H) + \frac{L^2}{2}A(F+G) + L\rho \frac{du_1}{dt} + \frac{L^2}{2}\rho B + L\rho u_1 A \tag{62}$$

$$u_1 = u_a + u_b \tag{63}$$

$$p_o - p_3 = \rho \frac{u_a^2}{2}(1+f_1) + u_aLF + u_aL[E(F+H)+\rho A] + \frac{L^2}{2}[A(F+G)+\rho B]$$

$$+ u_b[\rho u_a(1+f_1)+L(F+G)+s\rho L] \quad , \quad s = d(\cdot)/dt \tag{64}$$

$$p_o - p_3 = \rho \frac{u_a^2}{2} \cdot (1+f_1) + u_aLF + [\rho u_a(1+f_1) + L(F+G)]\,\Delta u_a \tag{65}$$

$$u_{a,n+1} = u_{a,n} + \frac{p_o - p_3 - \rho u_{a,n}^2 (1+f_1)/2 - u_{a,n} LF}{\rho u_{a,n}(1+f_1) + L(F+G)} \tag{66}$$

$$u_b = -\frac{u_aL[E(F+H) + \rho A] + L^2[A(F+G) + \rho B]/2}{(1+s\tau)[\rho u_a(1+f_1) + L(F+G)]} \tag{67}$$

$$\tau = \frac{\rho L}{\rho u_a(1+f_1) + L(F+G)} \tag{68}$$

$$\tau_o = \frac{\rho}{F+G} \tag{69}$$

$$p_o - p = p_1 - p + \rho \frac{u_1^2}{2}(1+f_1)$$

$$= \rho \frac{u_1^2}{2}(1+f_1) + xu_1[F + E(F+H) + \rho A + s\rho] + \frac{x^2}{2}[A(F+G) + \rho B]$$

$$p = p_o - \rho \frac{u_a^2}{2}(1+f_1) - xu_a F - xu_a [E(F+H) + \rho A] - \frac{x^2}{2}[A(F+G) + \rho B]$$

$$- u_b[\rho u_a(1+f_1) + x(F+G+s\rho)] \qquad (71)$$

DYNAMIC SEAL PARAMETERS

The fluid forces are obtained by integrating the pressure distribution of equation (71). First, the axial integration gives the radial force in equations (72), (75), (81), and (87); and second, the circumferential integration gives the total fluid force in equations (88) and (107). Equation (73) defines the average pressure p_a which does not contribute to the side force. Equation (74) defines the factor N of the variable velocity u_b as derived from equations (67) and (72). Equation (74) is further simplified by substituting with equations (68) and (69). The substitution of equation (67) in equation (72) yields equation (75) and the definitions of equations (76) through (84). The time constants of equations (68), (69), (80), (84), and (85) are ordered like the inequalities (86). The upper limit of equation (85) is derived by selecting a v/u ratio that minimizes the stator and the rotor frictions in F+G [equations (49), (50), and (69)]. The circumferential integration of equation (88) is vectorially accomplished to advantageously use the matrices of equations (89) and (90). The integration of the functions E, A, and B [equations (19), (43), and (56)] involves the function type of equation (91). The latter employs equation (89) to separate the angles α and β via the matrix product. The integrations of equations (92) lead to a diadic that, when integrated, yields a simple result. Equations (93) through (95) relate the polar and rectangular coordinates and their derivatives. Equations (96) through (98), the integrals of the functions E, A, and B, are transformed with equations (42) and (93) through (95); and $s = d(\cdot)/dt$ to rectangular coordinates, tacitly assuming Laplace transformed variables. Equations (87) and (96) through (98) yield the definitions of equations (99) through (107). Equations (102) through (106) give the frequency response of the dynamic parameters. The frequency response is due to the time constants τ, τ_a, and τ_b, which are small as indicated by the limit τ_u of equation (85) and inequalities (86). The frequency response is obtained with $s = j\omega$ and by replacing $1/(1+s\tau) = (1-s\tau)/(1+\omega^2\tau^2)$ and $s^3 = -s\omega^2$. The $(\omega\tau)^2$ terms are usually negligible; however, $(c\Omega)^2 m_c$ and τK_o are not [equations (102) and (107)]. The vector equation (107) is the dynamic model of the seal. The whirl driver is the off-diagonal elements that are proportional to the Couette factor c and the rotor speed Ω.

$$\int_o^L pdx = Lp_o - L\rho \frac{u_a^2}{2}(1+f_1) - \frac{L^2}{2}u_a F - \frac{L^2}{2}u_a[E(F+H) + \rho A] - \frac{L^3}{6}[A(F+G) + \rho B]$$

$$- Lu_b\left[\rho u_a(1+f_1) + \frac{L}{2}(F+G+s\rho)\right] \qquad (72)$$

$$p_a = p_o - \rho \frac{u_a^2}{2}(1+f_1) - \frac{L}{2} u_a F \tag{73}$$

$$N = \frac{1}{2(1+s\tau)} \cdot \frac{2\rho u_a(1+f_1)+L(F+G+s\rho)}{\rho u_a(1+f_1)+L(F+G)} = \frac{2+\tau(s-1/\tau_o)}{2(1+s\tau)} \tag{74}$$

$$\int_o^L pdx = Lp_a + L^2 u_a[E(F+H)+\rho A][N-1/2] + \frac{L^3}{2}[A(F+G)+\rho B][N-1/3] \tag{75}$$

$$N-1/2 = \frac{d}{2(1+s\tau)} \tag{76}$$

$$d = 1 - \frac{\tau}{\tau_o} = \tau\left(\frac{1}{\tau} - \frac{1}{\tau_o}\right) = \frac{\tau}{L} u_a(1+f_1) \tag{77}$$

$$N-1/3 = \frac{b}{2} \cdot \frac{1+s\tau_b}{1+s\tau} \tag{78}$$

$$b = \frac{4}{3} - \frac{\tau}{\tau_o} = \frac{\tau}{3}\left(\frac{4}{\tau} - \frac{3}{\tau_o}\right) = \frac{\tau}{3\tau_b} \tag{79}$$

$$\tau_b = \frac{\rho L}{4\rho u_a(1+f_1) + L(F+G)} \tag{80}$$

$$\int_o^L pdx = Lp_a + E\frac{L^2}{2} u_a d \cdot \frac{F+H}{1+s\tau} + \frac{A}{1+s\tau} \cdot \frac{L^2}{2}\left[\rho u_a d + \frac{L}{2}(F+G)\, b(1+s\tau_b)\right] + B\frac{L^3}{4}\rho b \frac{1+s\tau_b}{1+s\tau} \tag{81}$$

$$\rho u_a d + \frac{L}{2}(F+G)\, b(1+s\tau_b) = \tau\left[\frac{\rho}{L} u_a^2(1+f_1) + \frac{L}{6\tau_b}(F+G) + s\frac{L}{6}(F+G)\right] = a(1+s\tau_a) \tag{82}$$

$$a = \frac{\tau}{\tau_a} \cdot L\frac{F+G}{6} \tag{83}$$

$$\tau_a = \frac{\rho L^2 (F+G)}{\rho u_a (1+f_1)\,[6\rho u_a + 4L(F+G) + L^2 (F+G)^2} \tag{84}$$

$$\tau_u = \frac{4h_o}{u_a[\sqrt{f_s(f_s-g_s)} + \sqrt{f_r(f_r-g_r)}]} \tag{85}$$

$$\tau_u > \tau_o > \tau > \tau_b > \tau_a \tag{86}$$

$$\int_o^L pdx = Lp_a + E\frac{L^2}{2} u_a d \cdot \frac{F+H}{1+s\tau} + A\frac{L^2}{2} a \frac{1+s\tau_a}{1+s\tau} + B\frac{L^3}{4} \rho b \frac{1+s\tau_b}{1+s\tau} \tag{87}$$

$$\begin{bmatrix} F_y \\ F_z \end{bmatrix} = r \int_o^{2\pi} \left(\int_o^L pdx \right) Q_\beta \, id\beta \tag{88}$$

$$Q = Q_\alpha{}^T Q_\beta \tag{89}$$

$$Q_\beta = \begin{bmatrix} \cos\beta & -\sin\beta \\ \sin\beta & \cos\beta \end{bmatrix} \tag{90}$$

$$i^T(a_o I - b_o \Pi)Qi = a_o \cos(\beta-\alpha) + b_o \sin(\beta-\alpha) = i^T Q^T \begin{bmatrix} a_o \\ b_o \end{bmatrix} = i^T Q_\beta^T Q_\alpha \begin{bmatrix} a_o \\ b_o \end{bmatrix} \tag{91}$$

$$\int_o^{2\pi} i^T(a_o I - b_o \Pi)Qi \cdot Q_\beta \, id\beta = \int_o^{2\pi} Q_\beta \, ii^T Q_\beta{}^T \, d\beta \cdot Q_\alpha \begin{bmatrix} a_o \\ b_o \end{bmatrix} = \int_o^{2\pi} \begin{bmatrix} \cos^2\beta & \cos\beta\sin\beta \\ \sin\beta\cos\beta & \sin^2\beta \end{bmatrix} d\beta Q_\alpha \begin{bmatrix} a_o \\ b_o \end{bmatrix}$$

$$= \pi Q_\alpha \begin{bmatrix} a_o \\ b_o \end{bmatrix} = \pi(a_o I + b_o \Pi)Q_\alpha i \tag{92}$$

$$\begin{bmatrix} y \\ z \end{bmatrix} = h_o e Q_\alpha i \tag{93}$$

$$\begin{bmatrix} \dot{y} \\ \dot{z} \end{bmatrix} = h_o(\dot{e}I+\dot{\alpha}e\Pi)Q_\alpha i \tag{94}$$

$$\begin{bmatrix} \ddot{y} \\ \ddot{z} \end{bmatrix} = h_o[(\ddot{e}-\dot{\alpha}^2 e)I + (\ddot{\alpha}e+2\dot{\alpha}\dot{e})\Pi] \tag{95}$$

$$h_o \int_o^{2\pi} EQ_\beta \, id\beta = \pi h_o e Q_\alpha i = \pi \begin{bmatrix} y \\ z \end{bmatrix} \tag{96}$$

$$h_o \int_o^{2\pi} AQ_\beta \, id\beta = \pi h_o(\dot{e}I+\dot{\gamma}e\Pi)Q_\alpha i = \pi \begin{bmatrix} \dot{y} \\ \dot{z} \end{bmatrix} - \pi c\Omega\Pi \begin{bmatrix} y \\ z \end{bmatrix} = \pi(sI-c\Omega\Pi) \begin{bmatrix} y \\ z \end{bmatrix} \tag{97}$$

$$h_o \int_o^{2\pi} BQ_\beta \, id\beta = \pi h_o[(\ddot{e}-\dot{\gamma}^2 e)I + (\ddot{\alpha}e+2\dot{\gamma}\dot{e})\Pi] Q_\alpha i$$

$$= \pi \begin{bmatrix} \ddot{y} \\ \ddot{z} \end{bmatrix} - \pi(c\Omega)^2 \begin{bmatrix} y \\ z \end{bmatrix} - 2\pi c\Omega\Pi \begin{bmatrix} \dot{y} \\ \dot{z} \end{bmatrix} = \pi[(s^2 - (c\Omega)^2) I - s2c\Omega\Pi] \begin{bmatrix} y \\ z \end{bmatrix} \tag{98}$$

$$K_o = \frac{\pi r}{h_o} u_a^2 (1 + f_1) \tau \frac{L}{2} (F+H) \tag{99}$$

$$C_o = \frac{\pi r}{h_o} \frac{\tau}{\tau_a} \frac{L^3}{12} (F+G) \tag{100}$$

$$m_o = \frac{\pi r}{h_o} \frac{\tau}{\tau_b} \frac{L^3}{12} \rho = C_o \frac{\tau_a}{\tau_b} \tau_o \tag{101}$$

$$K = \frac{K_o}{1 + \omega^2 \tau^2} \tag{102}$$

$$C = \frac{C_o(1+\omega^2\tau\tau_a) + m_o\omega^2(\tau-\tau_b) - \tau K_o}{1+\omega^2\tau^2} \tag{103}$$

$$m = \frac{m_o(1+\omega^2\tau\tau_b) - C_o(\tau-\tau_a)}{1+\omega^2\tau^2} \tag{104}$$

$$C_c = \frac{C_o(1+\omega^2\tau\tau_a) + 2m_o\omega^2(\tau-\tau_b)}{1+\omega^2\tau^2} \tag{105}$$

$$m_c = \frac{m_o(1+\omega^2\tau\tau_b)}{1+\omega^2\tau^2} \tag{106}$$

$$\begin{bmatrix} F_y \\ F_z \end{bmatrix} = \begin{bmatrix} K-(c\Omega)^2 m_c + sC + s^2 m & c\Omega[C_c + s(m+m_c)] \\ -c\Omega[C_c + s(m+m_c)] & K-(c\Omega)^2 m_c + sC + s^2 m \end{bmatrix} \cdot \begin{bmatrix} y \\ z \end{bmatrix} \tag{107}$$

STABILITY

The dynamic models of turbomachines are far more complex than the simple model of Figure 1. The dynamic models consist of a sum of normal modes with gyroscopic moments and fluid forces added. The normal modes are the sum of resonators. The resonators are tuned to individual resonances, such as the critical speeds of the rotor. At one critical speed, one resonator dominates; and thus, the simple model of Figure 1 appears to be representative of the rotor behavior when the rotor mass is replaced by the generalized mass m_g and the suspension stiffness by the generalized stiffness K_g at the seal location. The stability is assessed by adding $K_g + s^2 m_g$ to the diagonal of the matrix in equation (107). The combined parameters are defined in equations (108) and (109). The determinant of the modified matrix of equation (107) gives the characteristic equation (110). (See Eq. 6.) The imaginary part of D = 0 yields the resonance of equation (111); and the real part, the stability limit of the inequalities (112) through (114). The ratio Ω_L/ω_o of equation (115) is approximately 1/c, because $C \doteq C_c$ and $\omega_o^2(m+m_c)$ is small. In other words, the Couette factor controls the speed limit.

$$K_r = K + K_g \tag{108}$$

$$m_r = m + m_g \tag{109}$$

$$D = [K_r - (c\Omega)^2 m_c]^2 + (c\Omega)^2 C_c^2 + s2[C(K_r - (c\Omega)^2 m_c) + (c\Omega)^2 C_c(m+m_c)]$$

$$+ s^2 [C^2 + 2(K_r - (c\Omega)^2 m_c)m_r + (c\Omega)^2 (m+m_c)^2] + s^3 2m_r C + s^4 m_r^2 = 0 \quad (110)$$

$$\omega_o^2 = \frac{K_r}{m_r} - (c\Omega)^2 \frac{m_c}{m_r} \quad (111)$$

$$2[K_r - (c\Omega)^2 m_c]^2 + (c\Omega)^2 C_c^2 < [K_r - (c\Omega)^2 m_c] C^2/m_r + 2[K_r - (c\Omega)^2 m_c]^2$$

$$+ [K_r - (c\Omega)^2 m_c](c\Omega)^2 (m+m_c)^2/m_r \quad (112)$$

$$(c\Omega)^2 C_c^2 < \omega_o^2 [C^2 + (c\Omega)^2 (m+m_c)^2] \quad (113)$$

$$\Omega < \frac{\omega_o}{c} \frac{C}{\sqrt{C_c^2 - \omega_o^2 (m+m_c)^2}} = \Omega_L \quad (114)$$

$$\frac{\Omega_L}{\omega_o} = \frac{C/c}{\sqrt{C_c^2 - \omega_o^2 (m+m_c)^2}} \quad (115)$$

NUMERICAL RESULTS

Table 1 compares a Rocketdyne analysis after Black for a uniform Couette flow factor c = 0.5 with the new analysis for equally polished seal surfaces of relative roughnesses $k_s/h_o = k_r/h_o = 0.002$. The results are similar and differ mostly at the fluid film stiffness. The difference is most likely due to Black's assumption of a dominant axial flow, while the new formulation is not thus restricted. Table 2 lists the recent design parameters for seals of the high pressure fuel turbopump's (HPFTP) first and second pump interstages, and the high pressure oxidizer turbopump's (HPOTP) inducer shroud. Table 3 gives the results for damping seals with rough strators of $k_s/h_o = 0.2$ and polished rotors of $k_r/h_o = 0.002$. A high roughness ratio is required because of the cubic root in Moody's friction equations (28) and (29). Table 3 demonstrates that speed limits of 2.8 and 3.9 times the first critical speed are feasible. The ratios Ω_L/ω_o are calculated with equation (115) for first critical speeds of 18,000 RPM and 15,000 RPM of the HPFTP and the HPOTP. respectively. An inlet loss factor of $f_1 = 0.5$ is applied in all cases. A comparison of Tables 1 and 3 shows that damping seals also have a lower leakage velocity u (70 percent).

TABLE 1. COMPARISON BETWEEN THE BLACK AND THE NEW MODEL

Dimensions	10^3 lb/in.		lb-s/in.		lb	ft/s	$\frac{1}{c}$
HPFTP Interstage Seals	K	$c\Omega C_c$	C	$c\Omega m_c$	m	u	
Black Model Rocketdyne Data 7/13/76	285	209	107	10.7	2.11	1004	2
New Model	404	205	93	6.5	0.56	1022	2

The comparison is for the straight smooth seal with a 3.14-in. diameter, 1.5 in. length, 37,360 RPM, and a relative roughness of $k_s/h_o = k_r/h_o = 0.002$ for the stator and the rotor.

TABLE 2. DESIGN PARAMETERS OF SEALS FOR THE HIGH PRESSURE FUEL TURBOPUMP (HPFTP) AND THE HIGH PRESSURE OXIDIZER TURBOPUMP (HPOTP) OF THE SPACE SHUTTLE MAIN ENGINE (SSME)

Dimensions	inch			psia		RPM	lb/cft	lb/ft-s
Seals	Gap	Dia.	Length	In	Out	Speed	Density	Viscosity
HPFTP First Interstage	0.0055	3.56	1.8	2432	288	36860	4.64	$1.06 \cdot 10^{-5}$
HPFTP Second Interstage	0.0055	3.56	1.8	4810	2557	36860	4.33	$0.86 \cdot 10^{-5}$
HPOTP Inducer Shroud	0.01	4.70	1.5	1824	433	30375	64.5	$8.00 \cdot 10^{-5}$
HPOTP Inducer Shroud	0.02	4.70	1.5	1824	433	30375	64.5	$8.00 \cdot 10^{-5}$

TABLE 3. DAMPING SEAL PARAMETERS

Dimensions	10^3lb/in.		lb-s/in.		lb	ft/s			10^3		10^{-6}s			10^{-3}	$\frac{1}{c}$	$\frac{\Omega_L}{\omega_o}$
Seals	K	$c\Omega C_c$	C	$c\Omega m_c$	m	u	v	w	R_s	R_r	τ	τ_b	τ_a	$(\omega_o\tau)^2$		
HPFTP First Interstage	340	182	182	4.9	1.3	660	142	573	271	316	24	16	15	2	4.0	3.9
HPFTP Second Interstage	358	179	181	4.5	1.2	703	140	573	333	383	23	15	14	2	4.1	3.9
HPOTP Inducer Shroud, 0.01 in. Gap	168	240	202	37	7.3	154	204	623	343	600	137	78	65	46	3.1	2.9
HPOTP Inducer Shroud, 0.02 in. Gap	116	123	101	23	3.2	217	195	623	783	1290	166	72	46	68	3.2	2.8

The stator and rotor roughnesses are $k_s/h_o = 0.2$ and $k_r/h_o = 0.002$, respectively, $\omega = 0$; and the critical speeds for the HPFTP and the HPOTP are 18,000 RPM and 15,000 RPM, respectively.

CONCLUSION

The dynamic and static seal parameters of seals with rough surfaces are derived without invoking a dominant axial flow. Whirl stability and leakage are shown to be controllable by employing a stator with a high surface roughness. The feasibility of damping seals is analytically demonstrated, but experimental verification is needed. The proposed seals are simple and should be readily applicable to turbomachinery. Speed limits can thus be raised, rotor vibrations reduced, bearing life improved, and costly shutdowns avoided.

REFERENCES

1. Barrett, L. E., Gunter, E. J., and Allaire, P. E.: Optimum Bearing and Support Damping for Unbalance Response and Stability of Rotating Machinery. Trans. ASME, Journal of Engineering for Power Vol. 100, pp. 89-94, January 1978.

2. Feder, E., Bansal, P. N., and Blanco, A.: Investigation of Squeeze Film Damper Forces Produced by Circular Centered Orbits. Trans. ASME, Journal of Engineering for Power Vol. 100, pp. 15-21, January 1978.

3. Childs, D. W.: The Space Shuttle Main Engine High-Pressure Fuel Turbopump Rotordynamic Instability Problem. Trans. ASME, Journal of Engineering for Power Vol. 100, pp. 48-57, January 1978.

4. Ek, M. C.: Solving Subsynchronous Whirl in the High-Pressure Hydrogen Turbomachinery of the SSME. AIAA Journal of Spacecraft and Rockets Vol. 17, No. 3, pp. 208-218, May-June 1980.

5. Black, H. F.: Effects of Hydraulic Forces in Annular Pressure Seals on the Vibrations of Centrifugal Pump Rotors. Journal Mechanical Engineering Science Vol. 11, No. 2, pp. 206-213, 1969.

6. Childs, D. W., Hendricks, R. C., and Vance, J. M.: Rotordynamics Instability Problems in High-Performance Turbomachinery. NASA Conference Publication 2133, Texas A&M University, May 12-14, 1980.

7. Massey, B. S.: Mechanics of Fluids. 3rd ed., p. 153, Van Nostrand Reinhold Co., New York, 1975.

8. Black, H. F., Allaire, P. E., and Barrett, L. E.: The Effect of Inlet Flow Swirl on the Dynamic Coefficients of High Pressure Annular Clearance Seals. 9th International Conference in Fluid Sealing, BHRA Fluid Engineering, Leeuwenhorst, The Netherlands, April 1981.

9. Moody, L. F.: Friction Factors for Pipe Flow. Trans. ASME, pp. 671-684, New York, November 1974.

10. Nyquist, H.: Regeneration Theory. Bell System Tech. Journal, Vol. 11, pp. 126-147, January 1932.

11. Murdock, J. W.: Fluid Mechanics and Its Application. pp. 269-271 and 124, Houghton Mifflin Co., Boston, 1976.

TECHNICAL REPORT STANDARD TITLE PAGE

1. REPORT NO.	2. GOVERNMENT ACCESSION NO.	3. RECIPIENT'S CATALOG NO.
NASA TP-1987		

4. TITLE AND SUBTITLE	5. REPORT DATE
Damping Seals for Turbomachinery	March 1982
	6. PERFORMING ORGANIZATION CODE
7. AUTHOR(S)	8. PERFORMING ORGANIZATION REPORT #
George L. von Pragenau	
9. PERFORMING ORGANIZATION NAME AND ADDRESS	10. WORK UNIT NO.
George C. Marshall Space Flight Center Marshall Space Flight Center, Alabama 35812	M-373
	11. CONTRACT OR GRANT NO.
	13. TYPE OF REPORT & PERIOD COVERED
12. SPONSORING AGENCY NAME AND ADDRESS	Technical Paper
National Aeronautics and Space Administration Washington, D.C. 20546	14. SPONSORING AGENCY CODE

15. SUPPLEMENTARY NOTES

Prepared by Systems Dynamics Laboratory, Science and Engineering

16. ABSTRACT

A rotor seal is proposed that restricts leakage like a labyrinth seal, but extends the stabilizing speed range beyond twice the first critical speed. The dynamic parameters are derived from bulk flow equations without requiring a dominant axial flow. The flow is considered incompressible and turbulent. Damping seals are shown to be feasible for extending the speed range of high performance turbomachinery beyond the limit imposed by conventional seals.

17. KEY WORDS	18. DISTRIBUTION STATEMENT
Rotor stability Couette flow Seal geometry Flow friction Flow continuity	Unclassified - Unlimited Subject category 07

19. SECURITY CLASSIF. (of this report)	20. SECURITY CLASSIF. (of this page)	21. NO. OF PAGES	22. PRICE
Unclassified	Unclassified	28	A03

MSFC - Form 3292 (Rev. December 1972)

For sale by National Technical Information Service, Springfield, Virginia 22161

NASA-Langley, 1982

National Aeronautics and
Space Administration

Washington, D.C.
20546

Official Business
Penalty for Private Use, $300

THIRD-CLASS BULK RATE

Postage and Fees Paid
National Aeronautics and
Space Administration
NASA-451

U.S.MAIL

6 1 1U,A, 031152 S00903DS
DEPT OF THE AIR FORCE
AF WEAPONS LABORATORY
ATTN: TECHNICAL LIBRARY (SUL)
KIRTLAND AFB NM 87117

NASA

POSTMASTER: If Undeliverable (Section 158 Postal Manual) Do Not Return